

Sulfation Rates of Cycled CaO Particles in the Carbonator of a Ca-Looping Cycle for Postcombustion CO₂ Capture

B. Arias, J. M. Cordero, M. Alonso, and J. C. Abanades

Instituto Nacional del Carbón, CSIC, C/Francisco Pintado Fe, No. 26, 33011 Oviedo, Spain

DOI 10.1002/aic.12745

Published online August 30, 2011 in Wiley Online Library (wileyonlinelibrary.com).

Calcium looping is an energy-efficient CO₂ capture technology that uses CaO as a regenerable sorbent. One of the advantages of Ca-looping compared with other postcombustion technologies is the possibility of operating with flue gases that have a high SO₂ content. However, experimental information on sulfation reaction rates of cycled particles in the conditions typical of a carbonator reactor is scarce. This work aims to define a semiempirical sulfation reaction model at particle level suitable for such reaction conditions. The pore blocking mechanism typically observed during the sulfation reaction of fresh calcined limestones is not observed in the case of highly cycled sorbents ($N > 20$) and the low values of sulfation conversion characteristic of the sorbent in the Ca-looping system. The random pore model is able to predict reasonably well, the CaO conversion to CaSO₄ taking into account the evolution of the pore structure during the calcination/carbonation cycles. The intrinsic reaction parameters derived for chemical and diffusion controlled regimes are in agreement with those found in the literature for sulfation in other systems. © 2011 American Institute of Chemical Engineers AIChE J, 58: 2262–2269, 2012

Keywords: sulfation kinetics, SO₂ capture, carbonation, Ca-looping, CO₂ capture

Introduction

Postcombustion CO₂ capture using CaO as a regenerable solid sorbent (or calcium looping, CaL) is a rapidly developing technology because of its potential to achieve a substantial reduction in capture cost and because of the energy penalties associated with more mature CO₂ capture systems.^{1,2} In a postcombustion CaL system, CO₂ from the combustion flue gas of a power plant is captured using CaO as sorbent in a circulating fluidized bed (CFB) carbonator operating between 600 and 700°C. The stream of partially carbonated solids leaving the carbonator is directed to the CFB calciner, where the solids are calcined, thereby regenerating the sorbent (CaO) and releasing the CO₂ captured in the carbonator. To calcine the CaCO₃ formed in the carbonator and to produce a highly concentrated stream of CO₂, coal is burned under oxy-fuel conditions at temperatures above 900°C in the calciner. One of the main distinctive characteristics of this process is its lower energy penalty, as operation at high temperatures allows for efficient heat integration of the full system in the power plant.^{3–8}

Another known benefit of CaL systems compared with other postcombustion technologies, such as amines, is the theoretical capability of operating with flue gases that have a high SO₂ content. This is because the calcined limestones present in carbonator and calciner reactors are known to be excellent desulfurization agents, and they are routinely used in many commercial scale power plants, including CFB

combustors (CFBC) (see review in Ref. 9). Although several recent works have investigated sulfation phenomena in CaL systems,^{10–17} there is a very little quantitative information on the sulfation rates of CaO in the carbonator and calciner reactor environments.

An important difference between sulfation studies with CFB combustors and sulfation studies with CaL systems concerns the typical range of conversion to CaSO₄ that can be expected of each of these systems. An obvious design target of any commercial flue gas desulfurization process is to make the most use of Ca and to achieve maximum conversion to CaSO₄. However, in a CaL system, there is generally a need for a large makeup flow of low-cost limestone to compensate for the decay in the sorbent's CO₂ carrying capacity along cycling. A mass balance for the recycling of Ca solids has shown¹⁸ that this leads to CaSO₄ contents well below 5 mol % in a CaL system, even when high sulfur content fuels are used. This has important implications for the debate of the effect of sulfur on CaL systems, because this low conversion of the Ca sorbent to CaSO₄ is well below the limit of conversion required to achieve the extensive pore plugging that is characteristic of highly sulfated particles (see review in Ref. 9). The purpose of this work, therefore, is to fully examine the sulfation phenomena associated with these low levels of conversion to CaSO₄.

Several models have been proposed for studying and describing heterogeneous sulfation reactions and pore plugging processes under different reaction controlled regimes and for different sorbents.^{19–25} The models increase in complexity when they need to quantify the diffusion phenomena of the reactants passing through plugged pores. However,

Correspondence concerning this article should be addressed to B. Arias at borja@incar.csic.es.

there is a general consensus concerning what happens in the initial stages of the reaction (low sulfation conversions). The first quantitative descriptions of the rate of reaction of SO_2 with CaO ^{26,27} established that, in the absence of diffusion through the pores of the particles, the reactivity of the sorbent toward SO_2 increases with the internal surface area. The overall reaction rate in these conditions is controlled by the chemical reaction at low values of sulfate conversion and by gas diffusion through a layer of CaSO_4 formed over the CaO sorbent that increases as the sulfation conversion increases. Regarding the effect of SO_2 concentration in gas phase, there is a general agreement that the reaction order ranges from 0.6 to 1.^{28,20,22,29} This background information should be valuable in modeling the sulfation rates of CaO particles in the typical conditions of CaL systems.

Another important difference between early works on the sulfation reaction of CaO in combustion environments and this study is to do with the range of temperatures. The most suitable mathematical models for describing the rate of sulfation of individual particles are usually fitted to the data obtained at temperatures characteristic of CFBC (around 850°C). However, these conditions differ considerably from those of a carbonator reactor working with a flue gas at lower temperatures (650°C).

Finally, it is necessary to take into account the special characteristics of the CaO particles cycling in a CaL capture system, where the reversible carbonation reaction of CO_2 with CaO has a strong impact on the textural properties of the material. It is well-known that CO_2 carrying capacity of CaO sorbents decays with number of calcinations/carbonations^{30,31} due to a sintering mechanism that drastically reduces the surface with the increasing number of cycles. In a scenario, where SO_2 is present in the flue gas entering the carbonator reactor, there is an additional deactivation of the CaO sorbent due to the formation of CaSO_4 . Several works have shown^{11–13,17} that SO_2 accelerates the decrease in CO_2 carrying capacity of a sorbent during cycling even when a low ratio of SO_2/CO_2 is used. One of the important conclusions of these cyclic tests is that the performance of limestones may differ considerably during sulfation in contrast to their similar behavior during carbonation.¹³ In their studies of the performance of calcium aluminate pellets during cocapture tests of CO_2 and SO_2 Manovic et al.¹⁷ showed that the deactivation of synthetic sorbents (calcium aluminate pellets) is greater than that of the natural limestone sorbent due to their higher reactivity toward SO_2 .

On the other hand, the sintering process of CaO under cyclic carbonation/calcination cycles can have a positive impact on sorbent use during sulfation. Some researchers have found that the sulfation behavior of CaO is enhanced (higher maximum sulfation conversions are achieved) during the calcination/carbonation cycles.^{10,13,14} This is because, the sintering of the particles during carbonation/calcination is accompanied by a widening of the pores to diameters of several 100 nm after extended (100) cycles.³² The opened structures formed during the calcination/carbonation cycles are then able to accommodate the bulky product layer of CaSO_4 , thus reducing the pore blocking mechanism which limits CaO conversion during sulfation. On the basis of this sorbent behavior, some researchers have suggested the idea of using the spent sorbent from carbonate looping as feedstock material for SO_2 retention in CFB boilers during coal combustion.^{13,15,16} This may be one of the reasons why most of the published data on

Table 1. Chemical Composition (wt %) of Limestones Used in this Work

	Al_2O_3	CaO	Fe_2O_3	K_2O	MgO	Na_2O	SiO_2	TiO_2
Compostilla	0.16	89.7	2.5	0.46	0.76	<0.01	0.07	0.37
Imeco	0.10	96.1	0.21	0.05	1.19	0.01	1.11	<0.05
Enguera	0.18	98.9	<0.01	0.03	0.62	0.00	0.43	0.02

the sulfation of spent sorbents is related with high temperatures typical of combustion temperatures (850–900°C) and there is a lack of experimental information on sulfation rates under carbonation temperatures (650°C).

The focus in this work is on the capture of SO_2 from the flue gas fed into the carbonator reactor, as this operates in conditions that may need to reconsider and reformulate the application of existing models at particle level to describe the sulfation reaction rates of CaO . Indeed, despite the large body of literature on the reaction of CaO with SO_2 in a wide range of conditions relevant to the operation of CFBCs, there is insufficient experimental information on sulfation reaction rates in the conditions characteristic of a carbonator reactor (i.e., particles that have undergone very different numbers of carbonation/calcination cycles, having substantially different textural properties and with expected conversions to CaSO_4 compared to that of CFBC systems). This work addresses this knowledge gap and presents what we believe to be the first results of an investigation to define a semiempirical sulfation reaction model at particle level suitable for the conditions characteristic of a carbonator reactor in a Ca -looping postcombustion system.

Experimental

Three different limestones with particle sizes in the range of 63–100 μm were used for this study. Their chemical composition is shown in Table 1. The calcination/carbonation cycling and the sulfation of the sorbents were experimentally studied using a thermo-gravimetric analyser (TGA) especially designed for carrying out long carbonation/calcination cycles, as described elsewhere.³³ This TG consists of a quartz tube installed in a two-zone furnace which is able to work at two different temperatures. The furnace can be moved up or down by means of a pneumatic piston and its position with respect to the sample allows a rapid change from calcination (950°C) to carbonation temperatures (650°C) and vice versa. The system is equipped with a microbalance that continuously measures the weight of the sample which is held in a platinum basket. The gas mixture ($\text{air}/\text{CO}_2/\text{SO}_2$) was prepared using mass flow controllers and was fed into the bottom of the quartz tube. The weight and temperature of the sample were continuously recorded on a computer.

The experimental procedure starts with the calcination carbonation cycling of the limestone for a certain number of cycles. During these tests, calcination was performed in air at 950°C and carbonation under 10% CO_2 in air at 650°C. After cycling, the sample temperature was allowed to stabilize for 10 min until a temperature of 650°C was reached. A mixture of SO_2 with air was then introduced into the quartz tube to begin sulfation. Tests were performed to establish the experimental conditions (sample mass and total gas flow) needed to avoid external diffusion effects. In the light of the results, the total volumetric flux was finally set to $2.25 \times 10^{-5} \text{ m}^3/\text{s}$, (corresponding to 0.05 m/s at 650°C). It was also

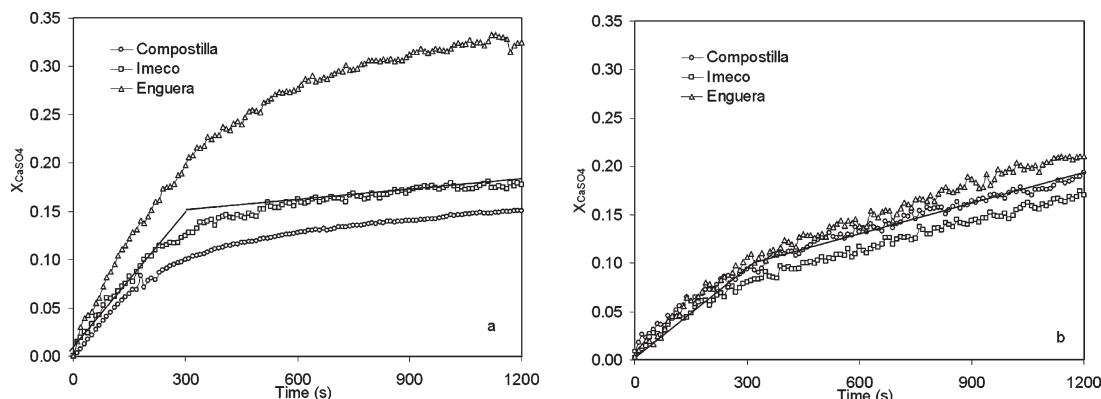


Figure 1. X_{CaSO_4} vs. time for limestones used in this work after the first calcination (a) and 50 calcination/carbonation cycles (b); $T = 650^\circ\text{C}$, SO_2 concentration = 500 ppmv.

established that a sample mass below 3 mg was necessary to eliminate external mass diffusion effects (i.e., at $T = 650^\circ\text{C}$ and 500 ppmv of SO_2). CaO conversion of the sorbent was calculated from the weight gain assuming that CaSO_4 would be the main product of the reaction between CaO and SO_2 under the experimental conditions of this work. After the end of each run, the samples were weighed using a different balance to check the accuracy of the TGA. A good agreement between both series of measurements was obtained in all cases.

Results and Discussion

Figure 1a shows the evolution of CaO conversion to CaSO_4 with time for limestones tested after a first calcination at a temperature of 650°C using 500 ppmv of SO_2 . As can be seen, the three sorbents exhibit an initial fast period followed by a second period with a lower reaction rate during which X_{CaSO_4} tends to stabilize to an almost constant value. In the case of the Compostilla and Imeco limestones, the sulfation rate of CaO fell sharply after 10 min of reaction, to a X_{CaSO_4} of 0.16 and 0.19, respectively. The reactivity of the Enguera limestone toward sulfation was much higher, yielding a X_{CaSO_4} of 0.35 at the end of the sulfation period. The drastic slowing down of the sulfation process has been reported widely in the literature and is attributed to pore blockage due to the different molar volumes of CaO and CaSO_4 (16.9 and $46.0\text{ cm}^3/\text{g}$, respectively).⁹

Figure 1b shows the CaO conversions to CaSO_4 after 50 calcination/carbonation cycles. As can be seen, the evolution of X_{CaSO_4} is quite similar for the three sorbents after cycling, despite the different behaviors of the freshly calcined limestones (Figure 1a). This is a clear indication of the strong effect of a large number carbonation/calcination cycles on the pore structure of CaO particles, irrespective of their origin, as revealed in previous studies on carbonation.³⁴

Certain similarities between Figures 1a and b are worth highlighting. On the one hand, the sulfation of the CaO cycled particles seems to maintain a certain transition (at about 300 s in these figures) between two stages in the rate of reaction. The fast reaction stage has a less inclined slope compared with the equivalent period in the fresh sorbent (Figure 1a), and this can be attributed to the smaller surface area of CaO particles after 50 carbonation/calcination cycles. Furthermore, the reduction in the reaction rate during the second stage is less pronounced in the case of the cycled sorbents (as the solid

lines show). Even more interesting is the fact that in Figure 1b, the reaction rate remains almost constant until the very end of the sulfation experiment, in contrast to what one would expect when the pore blockage mechanism takes place (as in Figure 1a). This behavior might be expected in view of the evolution of the sorbent surface, with cycling, toward one with a more opened texture and wider pores.^{13,17,32,35} A comparison of the experimental data in Figures 1a, b shows the importance of taking into account the evolution of sorbent texture during the calcination/carbonation cycles when modeling the sulfation process and determining the rate constants, as will be discussed later on.

Experiments with different particle sizes were performed to evaluate radial diffusion resistances throughout the pore network of the particles, focusing on the low level of sulfate conversion (fast reaction regions in Figure 1). Figure 2 shows the CaO conversion to CaSO_4 for the freshly calcined and cycled ($N = 20$) Compostilla limestone of two particle sizes, 63–100 μm and 400–600 μm , respectively. As can be seen, the reaction rates are similar for both sizes. This indicates that the SO_2 concentration is constant throughout the particle and that the sulfation rate can be described by means of a

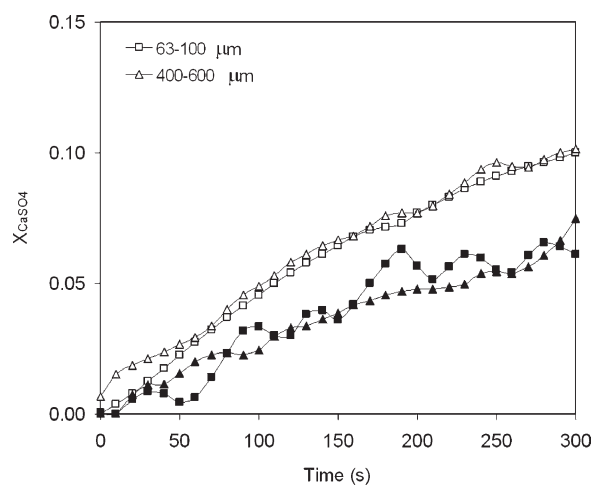


Figure 2. Effect of the particle size on the sulfation of CaO after the first calcination (empty symbols) and 20 calcination/carbonation cycles (filled symbols); $T = 650^\circ\text{C}$, SO_2 concentration = 500 ppmv.

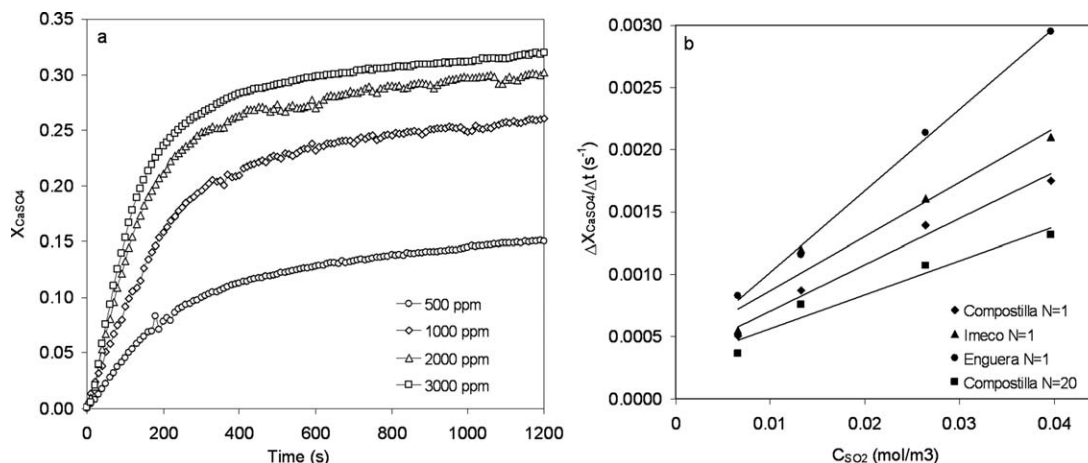


Figure 3. Effect of SO_2 concentration on X_{CaSO_4} for the fresh calcined Compostilla limestone ($N = 1$) (a) and the maximum reaction rate vs. SO_2 concentration (b) ($T = 650^\circ\text{C}$).

homogeneous model for these particle size ranges, common in CaL applications with CFB technology. However, this approach should always be reconsidered when using particles of a larger size in other systems.

To study the effect of SO_2 on the sulfation rate of CaO, tests with different concentrations were performed at a temperature of 650°C . The effect of the SO_2 concentration on X_{CaSO_4} in the case of Compostilla limestone after the first calcination cycle is shown in Figure 3a, where the SO_2 concentration ranges from 500 to 3000 ppmv. As can be seen, the SO_2 concentration has a marked effect on the slope of the initial stage of the sulfation process and on the final conversion of the sorbent after 20 min of reaction.

As mentioned earlier, different reaction orders can be found in the literature depending on the sulfation conditions. To determine the reaction order under the sulfation conditions tested in this work, the maximum sulfation rate ($\Delta X/\Delta t$) for the initial period (up to reaction times of 100 s) was represented against the SO_2 concentration. Figure 3b shows the results obtained for the slopes of the curves in the case of the fresh calcined Compostilla limestone. As can be seen, a good linearity is observed indicating a pseudofirst-order reaction respect to SO_2 . Figure 3b shows the results obtained for the other limestones ($N = 1$) and for the Compostilla limestone after 20 calcination/carbonation cycles confirming the first reaction order.

The aforementioned experimental results were interpreted in this work using the random pore model (RPM) proposed by Bhatia³⁶ and recently adapted to the carbonation reaction in CaL systems.^{37,38} This model has also been previously applied to freshly calcined limestones to study the diffusion and kinetic resistances involved in the sulfation process.²⁰ The RPM model has a general expression which is valid for solid–gas reactions and which is also applicable to porous systems with product layer resistance. Thus

$$\frac{dX}{dt} = \frac{k_s S C (1 - X) \sqrt{1 - \psi \ln(1 - X)}}{(1 - \varepsilon) \left[1 + \frac{\beta Z}{\psi} (\sqrt{1 - \psi \ln(1 - X)} - 1) \right]} \quad (1)$$

where

$$\beta = \frac{2k_s a \rho (1 - \varepsilon)}{b M_{\text{CaO}} D S} \quad (2)$$

and k_s is the rate constant for the surface reaction, S is the reaction surface area per unit of volume, ε is the porosity of the particles, D is the effective product layer diffusivity, and C is the SO_2 concentration. In Eq. 2, Ψ is a structural parameter that takes into account the internal particle pore structure which can be calculated as

$$\psi = \frac{4\pi L(1 - \varepsilon)}{S^2} \quad (3)$$

where L is the initial pore length in the porous system per unit of volume. For a chemically controlled reaction, the general rate expression from Eq. 1 can be simplified and integrated to yield the following equation [36]

$$\frac{1}{\psi} \left[\sqrt{1 - \psi \ln(1 - X)} - 1 \right] = \frac{k_s S C t}{2(1 - \varepsilon)} \quad (4)$$

On the other hand, when chemical kinetics and diffusion through the product layer are controlling the overall reaction rate, Eq. 1 can be integrated to the following equation

$$\frac{1}{\psi} \left[\sqrt{1 - \psi \ln(1 - X)} - 1 \right] = \frac{S}{(1 - \varepsilon)} \sqrt{\frac{D M_{\text{CaO}} C t}{2 \rho_{\text{CaO}} Z}} \quad (5)$$

Textural parameters, used as inputs in the RPM model (S , L , and ε), can be determined from experimental measurements.²⁰ In the case of cycled CaO, as the textural properties (S_N , L_N) change during cycling, their values for each cycle need to be known before the model can be applied. To avoid the need for experimental measurement of these parameters and in the absence of a detailed sintering model able to estimate the pore-size distribution during cycling, we adopted a similar methodology to that proposed by Grasa et al.³⁷ applying the RPM to the carbonation reaction of the cycled particles. Assuming that CaCO_3 forms a fairly constant layer at the end of the fast carbonation period³² and the total pore volume remains constant with the number of cycles, these authors proposed to determine S_N and L_N for each cycle, from the initial values (S_0 and L_0) and the maximum CO_2 carrying capacity of the sorbent (X_N) as follows

$$S_N = S_0 X_N \quad (6)$$

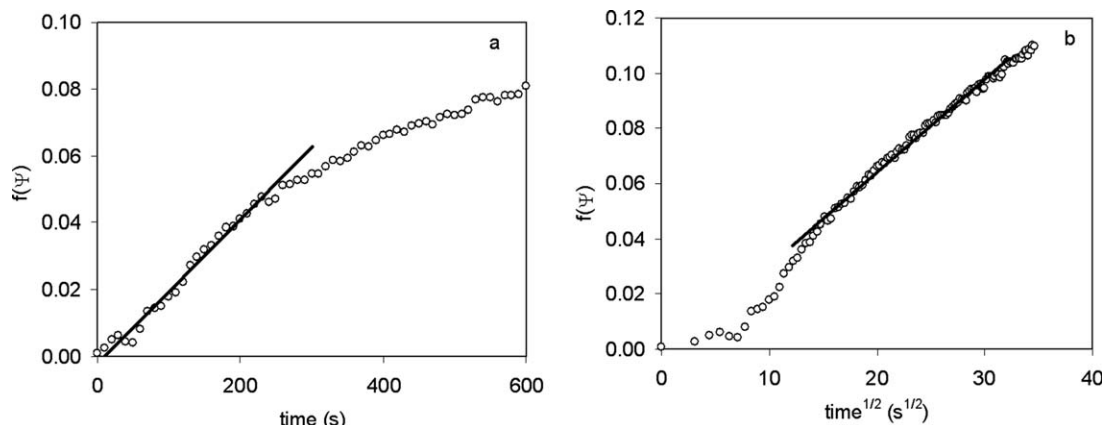


Figure 4. Fitting of Eq. 4 (a) and Eq. 5 (b) to the experimental data obtained for the Enguera limestone at $N = 20$ ($T = 650^{\circ}\text{C}$, SO_2 concentration = 500 ppmv).

$$L_N = L_0 X_N \frac{r_{p0}}{r_{pN}} \quad (7)$$

where S_0 and L_0 are the values corresponding to the initial fresh calcined limestones, and r_p is the pore radius (r_{p0} initial value, r_{pN} after N cycles). The maximum carrying capacity (X_N) in each cycle can be calculated using the following equation proposed by Grasa et al.³⁹

$$X_N = \left(\frac{1}{\frac{1}{(1-X_r)} + kN} + X_r \right) \quad (8)$$

where k is the deactivation constant, X_r is the residual conversion after an infinite number of cycles and N is the number of cycles. Values of $k = 0.52$ and $X_r = 0.075$ have been proven to be valid for a wide range of sorbents and carbonation conditions and have been used in this work. The values calculated for X_N by means Eq. 8 were compared with the experimental CO_2 carrying capacities obtained during TGA cycling and a good agreement was found. We estimated the initial surface area (S_0) of the fresh calcined limestones from the maximum CO_2 carrying capacity of the sorbent in the first cycle assuming the CaCO_3 layer thickness at the end of the fast reaction regimen to be 49 nm.³² This yields an initial value of $30 \times 10^6 \text{ m}^2/\text{m}^3$ assuming an initial CO_2 carrying capacity of 0.7 (using $N = 1$ in Eq. 8). The initial values of pore length (L_0) and porosity (ε) used for the three limestones were $4.16 \times 10^{14} \text{ m}/\text{m}^3$ and 0.46, respectively. These values were taken from a study of Grasa et al.³⁷ in which calcined Imeco limestone was characterized by mercury porosimetry.

Once the evolution of the surface area (S_N) and Ψ_N were calculated using the number of cycles, the reaction parameters, k_s and D , were determined by fitting Eqs. 4 and 5 to the experimental data. Figure 4 shows an example of the fitting of these equations to the experimental data obtained during the sulfation of Enguera limestone after 20 cycles of calcination/carbonation. Figures 4a, b represent the left-hand side of Eqs. 4 and 5 against time and $\text{time}^{1/2}$, respectively. From the slopes of the straight lines, k_s and D can be calculated. As can be seen from these figures, there is a clear threshold between the chemical and the diffusion controlled regime that can be easily identified for $f(\Psi) \sim 0.5$ which corresponds approximately to $X_{\text{CaSO}_4} = 0.10$. A similar marked threshold was observed for the other samples stud-

ied. This indicates that under these experimental conditions and with this particle size, the overall reaction rate is initially controlled by the chemical reaction rate that takes place over the entire surface of the sorbent. However, as the reaction proceeds, the surface is covered by a layer of CaSO_4 and diffusion through the product layer becomes the limiting step. No pore diffusion effects were detected in the experiments or used in the model.

Before discussing the values of k_s and D (shown in Table 2), it may be useful to test the suitability of this model for describing the evolution of X_{CaSO_4} with time. CaO conversion to CaSO_4 with reaction time can be calculated using the following equations which can be derived from Eqs. 4 and 5:

(a) for the chemically controlled regime

$$X = 1 - \exp \left[\frac{1 - \left(\frac{\tau}{2} \psi_N + 1 \right)^2}{\psi_N} \right] \quad (9)$$

(b) for the diffusion controlled regime

$$X = 1 - \exp \left[\frac{1}{\psi_N} - \frac{\left[\sqrt{1 + \beta Z \tau} - \left(1 - \frac{\beta Z}{\psi_N} \right) \right]^2 \psi_N}{(\beta Z)^2} \right] \quad (10)$$

where

$$\tau = \frac{k_s C S_N t}{(1 - \varepsilon)} \quad (11)$$

Figure 5 compares the experimental values with those calculated for Compostilla limestone for different numbers of cycles. In this figure, the transition between chemically and diffusion controlled regime has been obtained from the

Table 2. Calculated Kinetic Rate Parameters (k_s and D) for the Different Limestones at 650°C

Limestone	k_s ($\text{m}^4/\text{mol s}$)	D (m^2/s)	h_{CaSO_4} (nm)
Compostilla	4.32E-09	2.77E-12	8.6
Imeco	4.95E-09	2.41E-12	7.0
Enguera	5.63E-09	4.88E-12	9.9

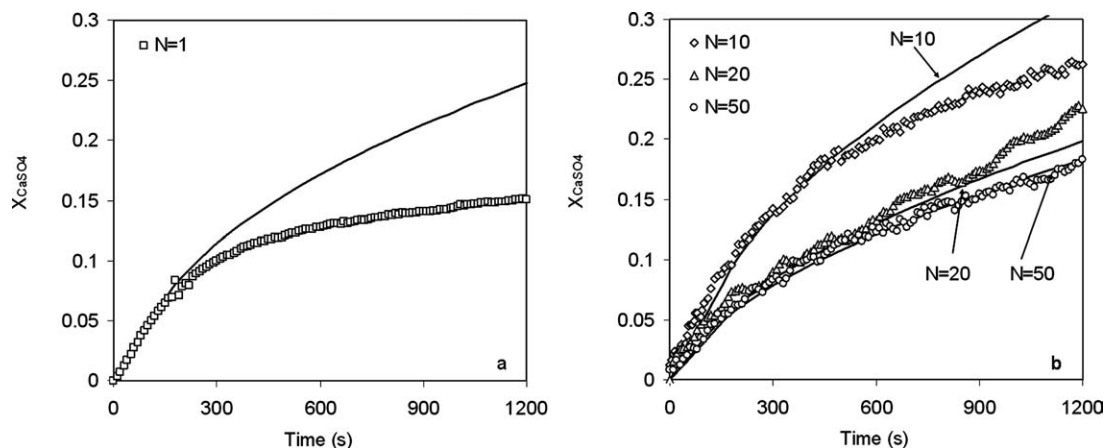


Figure 5. Comparison of experimental and calculated values of X_{CaSO_4} for Compostilla limestone with different numbers of cycles: (a) first cycle and (b) higher cycles ($T = 650^\circ\text{C}$, SO_2 concentration = 500 ppmv; calculated values: solid lines).

experimental results (typically around 120–180 s). Moreover, X_{CaSO_4} has been calculated using the k_s and D values derived for each cycle. As can be seen in the figure, the model only predicts satisfactorily the CaO conversion up to a value of ~ 0.10 in the case of the fresh calcined limestone ($N = 1$), which corresponds to a reaction time of around 4 min. From this point, the calculated values clearly over predict the experimental ones. By contrast, for the sorbent obtained after 10 calcination/carbonation cycles, the model is able to calculate the sorbent conversion up to values of $X_{\text{CaSO}_4} = 0.2$ which corresponds to a reaction time of ~ 10 min. In the case of the sorbent that has been cycled 20 and 50 times, the X_{CaSO_4} values calculated with the RPM model are in close agreement with the experimental ones over the entire reaction period.

The fact that the model correctly predicts the evolution of the sulfation conversion of the sorbent obtained after many carbonation/calcination cycles is a strong validation of the RPM model when applied to our results. It shows that the product layer of CaSO_4 is able to grow around the whole particle without experiencing any geometrical restrictions. The homogeneous model is not valid for particles derived from fresh calcined limestone because they undergo pore plugging as reaction proceeds. In the case of $N = 10$, the pore structure must be in an intermediate stage.

In a postcombustion Ca-looping system, most particles will have been cycling the system 10 s of times depending on the makeup flow ratio of fresh limestone.³⁴ Therefore, the assumption that the sulfation reaction progresses homogeneously in the particles, as indicated by Eqs. 1–8, will serve as an adequate approximation for practical reactor modeling purposes. A good agreement between the calculated values for cycled particles was found for each limestone, indicating the intrinsic nature of the values of k_s and D . By contrast, the best-fit values for the first cycle were clearly lower than that of the average values for all three limestones, especially in the case of the effective product layer diffusivity (D), which tends to be one order of magnitude lower. This can be explained by taking into account that the reaction surface in the particles has been calculated by means of Eqs. 6 and 8, which will tend to overestimate the reacting surface when small pores (that are prompt to CaSO_4 plugging) are present. The average values of k_s and

D for each limestone are summarized in Table 2. These have been calculated using the values of k_s and D calculated for each cycle, except those corresponding to the fresh calcined limestone ($N = 1$).

The values presented in Table 2 are in agreement with those found by Bhatia²⁰ for fresh calcined sorbents at temperatures of around 650°C . From the values of X_{CaSO_4} at which the transition between the chemical and diffusion controlled regime is observed and the surface area (S_N), it is possible to estimate the thickness of the product layer (h) at which the reaction becomes diffusion controlled by means of the following equation

$$h = \frac{X_{\text{CaSO}_4} \rho_{\text{CaO}} V_{M\text{CaSO}_4}}{S_N M_{\text{CaO}}} \quad (12)$$

The calculated values of h are shown in Table 2. An average CaSO_4 layer thickness of 8.5 nm is obtained. This average value can be used to estimate the sulfate conversion that marks the transition between the kinetic and the diffusion controlled regimes.

Although this work focused on the carbonator reactor, where the operation temperature will be fairly constant at around 650°C , we attempted to determine the influence of the temperature on the kinetic rate parameters by means of the Arrhenius equation

$$k_s = k_{s0} \exp(-E_{ak}/RT) \quad (13)$$

$$D = D_0 \exp(-E_{ad}/RT) \quad (14)$$

For this purpose, we performed tests at higher temperatures to determine k_s and D . However, diffusional resistances were observed during the tests at higher temperatures, which could not be avoided in our experimental setup. To overcome this

Table 3. Kinetic Parameters of Eqs. 13 and 146 for the Three Limestones

	Compostilla	Imeco	Enguera
k_{s0} ($\text{m}^4/\text{mol s}$)	6.38E-06	7.31E-06	8.31E-06
E_{ak} (kJ/mol)	56	56	56
D_0 (m^2/s)	1.71E-05	1.49E-05	3.02E-05
E_{ad} (kJ/mol)	120	120	120

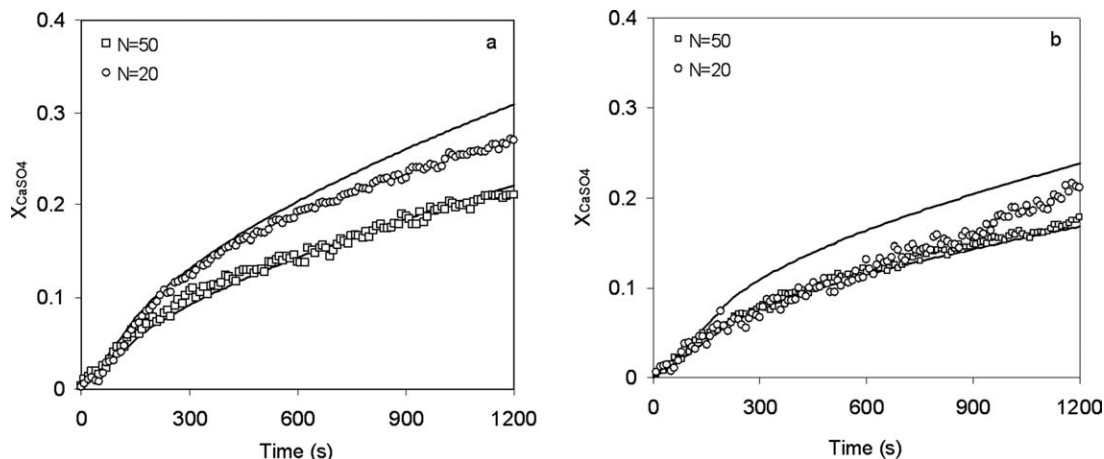


Figure 6. Comparison of experimental values of X_{CaSO_4} of Enguera (a) and Compostilla (b) limestones for $N = 20$ and 50 with those calculated by means of the model and the average values shown in Table 2 (solid lines); $T = 650^\circ\text{C}$, SO_2 concentration = 500 ppmv.

problem and to reduce the number of adjustable parameters, we determined the values of the pre-exponential factors, assuming an activation energy of 56 kJ/mol and 120 kJ/mol as calculated by Bhatia²⁰ for k_s and D , respectively. The results obtained are shown in Table 3.

Figure 6 shows the experimental evolution of X_{CaSO_4} with sulfation time together with those calculated using the average values of Table 2 and assuming a layer thickness of 8.5 nm for Enguera and Compostilla limestone with different numbers of cycles. As can be seen, there is reasonable agreement between the experimental and calculated values, confirming the suitability of the model for determining the sulfation rates of cycled sorbents.

When applying the RPM model to design Ca-looping systems, it will be found that for the typically low sulfation conversions of solids in these systems, the particles will react mainly under the chemical controlled regime. Therefore, the sulfation rate can be calculated using the simplified form of Eq. 1 for this regime together with the parameters reported in Table 3

$$\frac{dX}{dt} = \frac{k_s SC(1-X)\sqrt{1-\psi \ln(1-X)}}{(1-\varepsilon)} \quad (15)$$

The high reaction rate achieved for SO_2 capture under typical carbonator conditions in postcombustion Ca-looping systems, confirms that these reactors are suitable as SO_2 absorbers and as high-temperature CO_2 capture devices.

Conclusions

The RPM has been applied to study the sulfation behavior of cycled CaO particles at a temperature of 650°C (typical of carbonator reactors in Ca-looping CO_2 capture systems). Under these conditions, the sulfation proceeds through an initial chemically controlled step followed by second period where chemical reaction and diffusion through the product layer are the controlling resistances. Sulfation has been found to be a first reaction order with respect to SO_2 under the experimental conditions tested. The rate constants for surface reaction (k_s) between 4.32×10^{-9} and 5.63×10^{-9} $\text{m}^4/\text{mol s}$ were calculated at 650°C for the three limestones

used. The calculated values of effective product layer diffusivity (D) range from 2.43×10^{-12} to 4.88×10^{-12} m^2/s . These values are in agreement with those found in the literature under similar conditions. The results obtained with RPM indicate that cycled sorbents do not undergo pore plugging due to the growth of a layer of CaSO_4 (for reaction times of up to 20 min). For low CaO conversion ($X_{CaSO_4} < 0.05$), sulfation is a chemically controlled reaction. The high sulfation rates measured with highly cycled (carbonation/calcination) particles seem to indicate that postcombustion Ca-looping carbonator reactors will be effective reactors for capturing SO_2 from flue gases.

Acknowledgments

This work is partially funded by the European Commission (FP7-CaOling project).

Notation

- a, b = stoichiometric coefficients for sulfation reaction
- C = concentration of SO_2 , kmol/m^3
- D = effective product layer diffusivity, m^2/s
- D_0 = pre-exponential factor in Eq. 14, m^2/s
- E_{ak} = activation energy for the kinetic regime, kJ/mol
- E_{aD} = activation energy for the combined diffusion and kinetic regime, kJ/mol
- h = product layer thickness, m
- k = sorbent deactivation constant
- k_s = rate constant for surface reaction, $\text{m}^4/\text{mol s}$
- k_{s0} = pre-exponential factor in Eq. 13, $\text{m}^4/\text{mol s}$
- L = total length of pore system, m/m^3
- M = molecular weight, kg/kmol
- N = number of calcination/carbonation cycles
- r_{PN} = radius of the pore after N cycles, m
- S = reaction surface per unit of volume, m^2/m^3
- t = reaction time, s
- V_M = molar volume, m^3/kmol
- X_N = CaO molar conversion to CaCO_3 in each cycle
- X_{CaSO_4} = CaO molar conversion to CaSO_4
- X_r = residual CaO conversion
- Z = ratio volume fraction after and before reaction

Greek letters

- $\beta = 2k_s a \rho (1-\varepsilon)/M_{CaO} b D S$
- ε = porosity
- ρ = density, kg/m^3

$$\psi = 4\pi L(1 - \varepsilon)/S^2$$

$$\tau = k_s C S t / (1 - \varepsilon)$$

Literature Cited

- Anthony EJ. Solid looping cycles: a new technology for coal conversion. *Ind Eng Chem Res.* 2008;47:1747–1754.
- Blamey J, Anthony EJ, Wang J, Fennel PS. The calcium looping cycle for large-scale CO₂ capture. *Progr Energ Combust Sci.* 2010;36:260–279.
- Shimizu T, Hiramata T, Hosoda H, Kitano K, Inagaki M, Tejima K. A twin fluid-bed reactor for removal of CO₂ from combustion processes. *Trans IChemE.* 1999;77:62–68.
- Romeo LM, Abanades JC, Escosa JM, Paño J, Jiménez A, Sánchez-Biezma A, Ballesteros JC. Oxyfuel carbonation/calcination cycle for low cost CO₂ capture in existing power plants. *Energ Convers Manag.* 2008;49:2809–2814.
- Romano M. Coal-fired power plant with calcium oxide carbonation for post-combustion CO₂ capture. *Energy Procedia.* 2009;1:1099–1006.
- Ströle J, Lasheras A, Galloy A, Eppe B. Simulation of the carbonate looping process for post-combustion CO₂ capture from a coal-fired power plant. *Chem Eng Technol.* 2009;32:435–442.
- Yongping Y, Rongrong Z, Liqiang D, Kavosh M, Patchigolla K, Oakley J. Integration and evaluation of a power plant with a CaO-based CO₂ capture system. *Int J Greenhouse Gas Control.* 2010;4: 603–612.
- Martínez I, Murillo R, Grasa G, Abanades JC. Integration of Ca looping system for CO₂ capture in existing power plants. *AIChE J.* 2011;57:2599–2607.
- Anthony EJ, Granatstein DL. Sulfation phenomena in fluidized bed combustion systems. *Progr Energ Combust Sci.* 2001;27:215–236.
- Li Y, Buchi S, Grace JR, Lim CJ. SO₂ removal and CO₂ capture by limestone resulting from calcination/sulfation/carbonation cycles. *Energy Fuels.* 2005;19:1927–1934.
- Ryu HJ, Grace JR, Lim CJ. Simultaneous CO₂/SO₂ capture characteristics of three limestones in a fluidized-bed reactor. *Energy Fuels.* 2006;20:1621–1628.
- Sun P, Grace JR, Lim CJ, Anthony EJ. Removal of CO₂ by calcium-based sorbents in presence of SO₂. *Energy Fuels.* 2007; 21:163–170.
- Grasa GS, Alonso M, Abanades JC. Sulfation in a carbonation/calcination loop to capture CO₂. *Ind Eng Chem Res.* 2008;47:1630–1635.
- Manovic V, Anthony EJ. Sequential SO₂/CO₂ capture enhanced by steam reactivation of CaO-based sorbent. *Fuel.* 2008;87:1564–1573.
- Manovic V, Anthony EJ, Loncarevic D. SO₂ retention by CaO-based sorbent spent in CO₂ looping cycles. *Ind Eng Chem Res.* 2009;48: 6617–6632.
- Pacciani R, Müller CR, Davidson JF, Dennis JS, Hayhurst AN. Performance of novel synthetic Ca-based sorbent suitable for desulfurizing flue gases in a fluidized bed. *Ind Eng Chem Res.* 2009;48: 7016–7024.
- Manovic M, Anthony EJ. Competition of sulphation and carbonation reactions during looping cycles for CO₂ capture by CaO-based sorbents. *J Phys Chem A.* 2010;114:3397–4002.
- Abanades JC, Anthony EJ, Wang J, Oakley JE. Fluidized bed combustion systems integrating CO₂ capture with CaO. *Environ Sci Technol.* 2005;39:2861–2866.
- Georgakis C, Chang CW, Szekely J. A changing grain size model for gas–solid reactions. *Chem Eng Sci.* 1979;34:1072–1075.
- Bhatia SK, Perlmutter DD. The effect of pore structure on fluid–solid reactions: application to the SO₂–lime reaction. *AIChE J.* 1981;27:226–234.
- Borgwardt RH, Bruce KR. Effect of specific surface area on the reactivity of CaO with SO₂. *AIChE J.* 1986;32:239–246.
- Borgwardt RH, Bruce KR, Blake J. An investigation of product-layer diffusivity for CaO sulfation. *Ind Eng Chem Res.* 1987;26:1993–1998.
- Dennis JS, Hayhurst AN. Mechanism of the sulphation of calcined limestone particles in combustion gases. *Chem Eng Sci.* 1990;45: 1175–1187.
- Hartman M, Coughlin RW. Reaction of sulfur dioxide with limestone and the grain model. *AIChE J.* 1976;22:490–498.
- Adánez J, García-Labiano F, Fierro V. Modelling for the high-temperature sulphation of calcium-based sorbents with cylindrical and plate-like geometries. *Chem Eng Sci.* 2000;55:3665–3683.
- Borgwardt RH. Kinetics of the reaction of SO₂ with calcined limestone. *Environ Sci Technol.* 1970;4:59–61.
- Hartman M, Coughlin RW. Reaction of sulfur dioxide with limestone and the influence of pore structure. *Ind Eng Chem Process Des Dev.* 1974;13:248–253.
- Pigford RL, Sliger G. Rate of diffusion-controlled reaction between gas and a porous solid sphere. Reaction of SO₂ with CaCO₃. *Ind Eng Chem Process Des Dev.* 1973;12:85–91.
- Adánez J, Gayán P, García-Labiano F. Comparison of mechanistic models for the sulfation reaction in a broad range of particle sized of sorbents. *Ind Eng Chem Res.* 1996;35:2190–2197.
- Curran GP, Fink CE, Gorin E. CO₂ acceptor gasification process. Studies of acceptor properties. *Adv Chem Ser.* 1967;69:141–161.
- Barker R. Reversibility of the reaction CaCO₃ = CaO + CO₂. *J Appl Chem Biotechnol.* 1973;23:733–742.
- Alvarez D, Abanades JC. Determination of the critical product layer thickness in the reaction of CaO with CO₂. *Ind Eng Chem Res.* 2005;44:5608–5615.
- González B, Grasa GS, Alonso M, Abanades JC. Modeling of the deactivation in a carbonate loop at high temperatures calcination. *Ind Eng Chem Res.* 2008;45:9256–9262.
- Abanades JC. The maximum capture efficiency of CO₂ using a carbonation/calcination cycle of CaO/CaCO₃. *Chem Eng J.* 2002;60:303–306.
- Abanades JC, Álvarez D. Conversion limits in the reaction of CO₂ with lime. *Energy Fuels.* 2003;17:308–315.
- Bhatia SK, Perlmutter DD. A random pore model for fluid–solid reactions. I. Isothermal, kinetic control. *AIChE J.* 1980;26:379–386.
- Grasa G, Murillo R, Alonso M, Abanades JC. Application of the random pore model to the carbonation cyclic reaction. *AIChE J.* 2009;55:1246–1255.
- Arias B, Abanades JC, Grasa GS. An analysis of the effect of carbonation conditions on CaO deactivation curves. *Chem Eng J.* 2011; 167:255–261.
- Grasa GS, Abanades JC. CO₂ capture capacity of CaO in long series of carbonation/calcination cycles. *Ind Eng Chem Res.* 2006;45: 8846–8851.

Manuscript received May 18, 2011, and revision received July 25, 2011.